

# Deposit Effects on Plate-haptic Rotationally Asymmetric Refractive Multifocal Intraocular Lens with +1.5D Addition Power

Takashi MATSUSHIMA and Kenji KAWAI

*Department of Ophthalmology, Tokai University School of Medicine*

(Received March 9, 2023; Accepted July 13, 2023)

**Objective:** To evaluate the optical performance of plate-haptic rotationally asymmetric refractive multifocal intraocular lenses (IOLs) with +1.5 D addition power by reproducing calcium deposition using rabbit eyes.

**Methods:** Five IOLs (LS-313 MF15 [Santen/Teleon], W-60R [Santen], NS1 [KOWA], SY60WF [Alcon], and NS-60YS [NIDEK]) with varying water content were randomly implanted in rabbit eyes. Cell proliferation in the lens capsule and deposits on the IOL surface were confirmed with a slit lamp. The surface deposits were stained with alizarin red, and IOL transmittance was measured with a spectrophotometer. IOL storage solutions were analyzed using inductively coupled plasma mass spectrometry to confirm the presence of calcium.

**Results:** Slit-lamp observations revealed abundant cellular proliferation on all IOLs. Granular deposits, unlike proliferating cells, were observed on LS-313 MF15 lenses two months after surgery, increasing over time, and stained red. The transmittance of LS-313 MF15 decreased in correlation with the stained area. Calcium was detected in all IOL storage solutions; however, deposits were confirmed only on the LS-313 MF15 surface, indicating decreased transmittance.

**Conclusion:** These findings can facilitate predicting deposition on IOLs in clinical settings and selecting IOL materials for long-term stability. The long-term use of LS-313 MF15 IOLs requires further verification to avoid post-surgical extraction.

**Key words:** Intraocular lenses, water content, rabbit eyes, opacification, calcification

## INTRODUCTION

Plate-haptic rotationally asymmetric refractive multifocal intraocular lenses (IOLs) with +1.5 D addition power (Lentis Comfort LS-313 MF15 [Santen/Teleon]) are fabricated using a hydrophilic material with hydrophobic surface properties. Combining the +1.5 D added power with a unique design reduces unpleasant dysphotopsia and provides good distant and intermediate visual acuity [1]. The HydroSmart IOL (Oculentis BV), constructed from the same material as this IOL, exhibits calcium deposition [2]. In recent years, calcium deposition has also been reported in the LS-313 MF15 lenses [3, 4].

Calcium deposition is a process by which calcium ions present in the aqueous humor are deposited on the IOL surface as crystals of calcium phosphate. Since calcium phosphate blocks light transmission, calcium deposition is a serious complication that can lead to IOL removal [5-7]. Thus, considering the long-term stability and maintenance of the transparency of IOL materials, evaluating their potential susceptibility to calcium deposition is of great importance.

In addition to calcium deposition, glistening and subsurface nano-glistening reduce the transparency of IOL materials [8]. In recent years, new hydrophobic acrylic materials with a higher water content than conventional hydrophobic acrylic materials have been developed to suppress glistening, with reports indicat-

ing good results [9-13].

Glistening refers to bright spots caused by aqueous humor compounds diffusing in minute amounts into IOLs [14]. Increasing the water content of acrylic materials before implantation inhibits the formation of these bright spots. Generally, increasing the proportion of hydrophilic functional groups in a material increases its water content.

Compared with hydrophobic functional groups, hydrophilic functional groups are more susceptible to adsorbing ionic components. Therefore, high-water-content hydrophobic acrylic materials have an increased proportion of hydrophilic functional groups, and a large quantity of ionic compounds in the aqueous humor may be adsorbed more readily, leading to calcium deposition.

Thus, we attempted to reproduce calcium deposition in vitro on plate-haptic rotationally asymmetric refractive multifocal IOLs with +1.5 D addition power by implanting them in rabbit eyes. As controls, new and conventional hydrophobic acrylic materials were selected, and we observed deposit formation on the IOL surface. Moreover, we investigated the effect of the deposits on the optical performance of the IOLs using transmittance as an index.

## MATERIALS AND METHODS

### Rabbit eye implantation trial

Twenty-five eyes of 13 Japanese white rabbits

**Table 1** Properties of implanted lenses

Manufacturer	Teleon/Santen	Santen	KOWA	Alcon	NIDEK
Product name	Lentis comfort	Eternity	Avansee	Clareon	Nex-Acri AA 1P
Model name	LS-313 MF15	W-60R	NSI	SY60WF	NS-60YS
Hydrophobicity/ Hydrophilicity	Hydrophilic	Hydrophobic	Hydrophobic	Hydrophobic	Hydrophobic
Material	Hydrophilic acrylic material with a hydrophobic surface	Copolymer of hydroxyethyl methacrylate, polyethylene glycol phenyl ether acrylate, and styrene crosslinked with ethylene glycol dimethacrylate	Copolymer of phenoxy-ethyl-acrylate and ethyl-acrylate	Hydrophobic acrylic polymer	Copolymer of butyl acrylate and phenoxy-ethyl-acrylate
Water content (%)	25	4	< 2.0	1.5	< 0.1
Glass transition temperature (°C)	NA	NA	15	9.10 ± 0.27	3.6
Refractive index	1.46	1.54	1.519	1.55	1.52

NA: data not available in the literature or on request from the manufacturer.

weighing 2.1–2.6 kg were used in our experiment. Five IOL models with differing water contents (LS-313 MF15 [Santen, Osaka, Japan/Teleon Surgical BV, Spankeren, Netherlands], W-60R [Santen, Osaka, Japan], NSI [KOWA, Nagoya, Japan], SY60WF [Alcon, Fort Worth, TX, United States], and NS-60YS [NIDEK, Gamagori, Japan]) were selected [2, 15–18] (Table 1).

All lenses had a power of 20.0 D. Five lenses of each model were randomly implanted to minimize the effects of individual differences between rabbits. This study was approved by the Animal Experimental Committee of NIDEK Co., LTD. (approval number 19C009). All procedures were conducted following international guidelines for the care and use of laboratory animals. In accordance with the Association for Research in Vision and Ophthalmology guidelines, all implantations were performed by the same surgeon.

After achieving mydriasis with 0.5% tropicamide and 0.5% phenylephrine hydrochloride drops (Mydrin P, Santen Pharmaceutical, Osaka, Japan), the rabbits were placed under general anesthesia using an intramuscular injection of a 6:1 mixture of 5% ketamine (Ketalar, Daiichi Sankyo, Tokyo, Japan) and 2% xylazine (Selactar, Bayer Yakuhin, Osaka, Japan) (1.0 mL/kg). Their eyeballs were washed with a 5-fold dilution of 0.2% polyvinyl alcohol and 8% iodine solution (PA IODO Ophthalmic and Eye washing Solution, Nitten Pharmaceutical, Nagoya, Japan). Subsequently, 0.4% oxybuprocaine hydrochloride (Benoxil, Santen Pharmaceutica, Osaka, Japan) was used as eye drop anesthesia. A side port was constructed using a micro-vitreoretinal blade, and the anterior chamber was filled with a high molecular-weight ophthalmic viscosurgical device (OVD). After continuous curvilinear capsulotomy (CCC; approximately 5 mm) was performed using capsulorhexis forceps, a 2.4-mm incision was made in the cornea. Subsequently, hydro-dissection was performed, and the crystalline lens was removed by aspiration. The lens capsule and anterior chamber were filled with a high molecular-weight OVD, and the injector suggested by each manufacturer (WJ-60MII [Santen], YP2.2R [KOWA], AU00T0 [Alcon], and NSP-1 [NIDEK]) was used for IOL insertion. After removing the high molecular-weight OVD, the incision was sutured using 10-0 nylon, and the surgery

was completed. Postoperatively, drops of 0.1% beta-methasone phosphate sodium (Rinderon, Shionogi, Osaka, Japan), 0.3% ofloxacin (Tarivid, Santen Pharmaceutica, Osaka, Japan), and 0.1% nepafenac (Nevanac, Novartis, Tokyo, Japan) were administered in each eye thrice daily for three weeks.

Follow-up observations were recorded at one, two, and four weeks postoperatively, and every month thereafter, for six months, to assess cell proliferation in the capsule (posterior capsular opacification, PCO) and deposition on the IOLs using a slit lamp (SL130, Carl Zeiss, Oberkochen, Germany) and anterior segment optical coherence tomography (OCT; SS-1000 CASIA, TOMEY, Nagoya, Japan) after pupil dilatation with 0.5% tropicamide and 0.5% phenylephrine hydrochloride drops (Mydrin P, Santen Pharmaceutical, Osaka, Japan). The experiment was concluded if severe inflammation was observed in the eyes; only cases that completed six months of observation were deemed successful.

### **Eyeball and IOL extraction**

After six months of follow-up, an excess of 6.48% pentobarbital sodium (1 mL/kg; somnopentyl, Kyoritsu Seiyak, Tokyo, Japan) was injected intravenously, and the eyeballs were extracted and stored on ice in physiological saline for observation. IOL fixation and cell proliferation within the lens capsule were examined via the Miyake–Apple view. The IOLs were extracted from the lens capsule under a microscope and washed in physiological saline using an ultrasonic washer for 15 min to remove the cells that had proliferated on the surface [19].

### **Evaluation of extracted IOLs**

The excised IOLs were stored in 0.9% saline (Otsuka Normal Saline, Otsuka Pharmaceutica, Tokyo, Japan) at 4°C until evaluation.

### **Alizarin red staining**

An alizarin red S staining solution (1%) was prepared by titrating 1 g alizarin red S (FUJIFILM Wako Pure Chemical Corporation, Osaka, Japan) dissolved in 100 mL ultrapure water with an aqueous solution of ammonia (0.1 mL of 28% aqueous ammonia and 100

**Table 2** Number of implanted lenses of each type and the observation period in each rabbit

Model	At implantation		Follow-up observation		Successful cases: 6 months post-operation (number of lenses)
	Number of lenses		4 months post-operation (number of lenses)	5 months post-operation (number of lenses)	
LS-313 MF15	5		1	0	4
W-60R	5		0	2	3
NS1	5		2	1	2
SY60WF	5		2	0	3
NS-60YS	5		2	1	2

mL water) to achieve a pH of 4.1–6.4. Extracted IOLs were washed with physiological saline, subjected to ultrasound waves for 15 min [19], washed with ultrapure water, and stained by immersion in the alizarin red S staining solution for 2 min. Stained IOLs were washed with ultrapure water four times for 30 s each and observed under a stereomicroscope (SMZ1500, Nikon, Tokyo, Japan). Using ImageJ (Ver1.52v, US National Institutes of Health, Bethesda, Maryland, United States), the percentage of red-stained area for each lens was calculated, and the mean values were compared. The correlation between the dyed area ratio and the water content of the material was evaluated by regression analysis. The water content of the material used was adopted from previously reported values or according to the manufacturer's nominal value (Table 1).

#### Quantitative estimation of calcium

The extracted IOLs were stored in physiological saline. The calcium present in these storage solutions was quantified using inductively coupled plasma mass spectrometry (ICP-MS) (8800, Agilent Technologies, Palo Alto, California, United States).

#### Measurement of transmittance

Spectral transmittance of the extracted IOLs was measured using a spectrophotometer (UV-2600, SHIMADZU CORPORATION, Kyoto, Japan). The measured wavelengths ranged from 300–800 nm, and the transmittance values were compared against those obtained from non-implanted IOLs of the same type. The decrease in transmittance at wavelengths of 500 and 800 nm (transmittance of the extracted IOL/transmittance of the non-implanted IOL)/transmittance of the non-implanted IOL) was calculated, and the correlation between the area stained with alizarin red and the decrease in transmittance was evaluated using regression analysis.

## RESULTS

#### Follow-up observations (initially after surgery–five months post-surgery)

Each of the five types of IOLs, namely, LS-313 MF15, W-60R, NS1, SY60WF, and NS-60YS, were randomly implanted binocularly in 25 rabbit eyes successfully, without any complications. At the end of the surgery, the CCC opening was covered 360° by the optical portion of each IOL.

Mild PCO was observed in the remaining cortex of the lens capsule one week postoperatively. The CCC

opening was observed outside the optical portion of the IOL in all cases. PCO was least apparent in the eyes with LS-313 MF15 lenses. Although the degree of PCO in W-60R, NS1, SY60WF, and NS-60YS was slightly higher than that in LS-313 MF15, there was no difference in the PCO between these lenses.

At one-month post-surgery, PCO had further increased in all cases; at two months, cells had proliferated onto the anterior surface of the IOL, the incised area in the anterior capsule, and within the anterior chamber. White granular deposits that differed from the proliferating cells were observed on the LS-313 MF15 lenses beginning at two months postoperatively; the number of deposits increased over time.

Cells that proliferated in front of the IOL were in contact with the iris and cornea. Iris hyperemia, edema, and corneal cloudiness were confirmed, and these symptoms gradually worsened. When recovery was judged unlikely, the cases were considered complete at four and five months postoperatively. Cases completing six months of postoperative evaluation were eligible for analysis (LS-313 MF15 [n = 4], W-60R [n = 3], NS1 [n = 2], SY60WF [n = 3], and NS-60YS [n = 2]; Table 2).

#### Pre-extraction evaluation

Slit lamp images taken before ocular extraction (six months postoperatively) revealed abundant cellular proliferation inside the lens capsule of all IOL-implanted eyes. In addition, varying degrees of iris hyperemia, corneal opacity, and angiogenesis, possibly due to the force exerted by the proliferating cells on the peripheral tissues, were observed in all eyes (Fig. 1, upper images). Anterior segment OCT revealed a thick cellular layer in contact with the iris surface anterior and posterior of the IOL in the lens capsule (Fig. 1, middle images). Miyake–Apple view images revealed that the haptics of all IOLs were fixed to the equator of the lens capsule. In all IOL-implanted eyes, rampant cellular proliferation and fibrin adhesion were observed inside the lens capsule. Compared with the W-60R, NS1, SY60WF, and NS-60YS lenses, slightly less cellular proliferation occurred with LS-313 MF15 lenses. Moreover, no significant differences in cellular proliferation were observed among W-60R, NS1, SY60WF, and NS-60YS IOLs (Fig. 1, lower images).

In addition, granular deposits with a morphology distinctly different from that of proliferating cells were observed on the anterior surface of the LS-313 MF15 IOL (Fig. 2). There were no granular deposits on the W-60R, NS1, SY60WF, and NS-60YS IOLs.

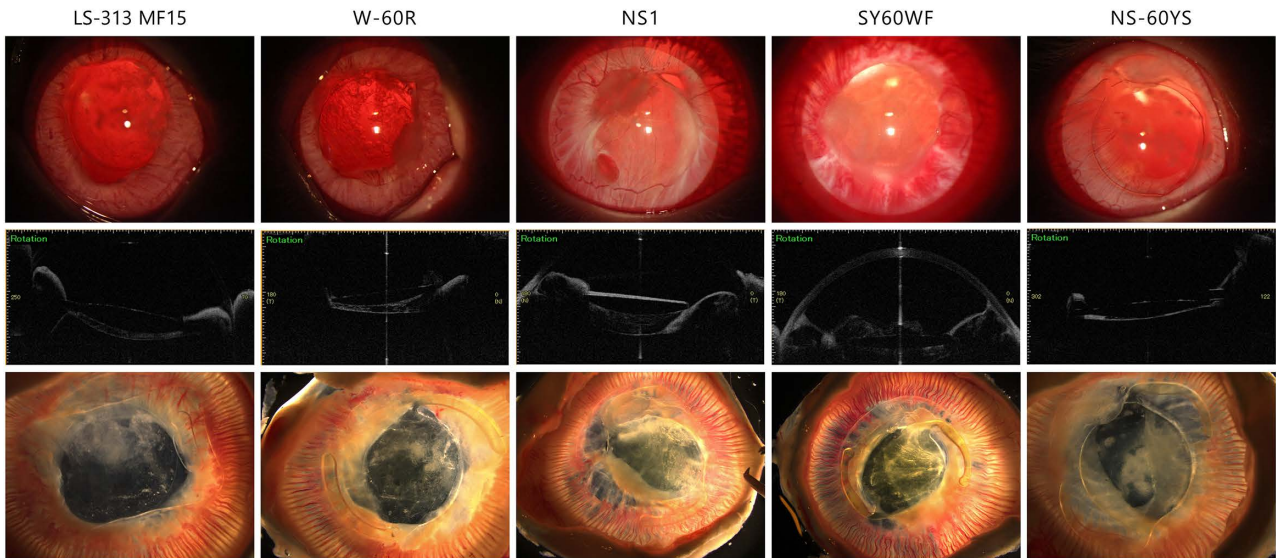


**Fig. 1** Representative examples of each lens type six months postoperatively  
 Upper: slit lamp images, middle: anterior segment optical coherence tomography, lower: Miyake-Apple view.  
 Rampant cellular proliferation was observed inside the lens capsule for all lens types

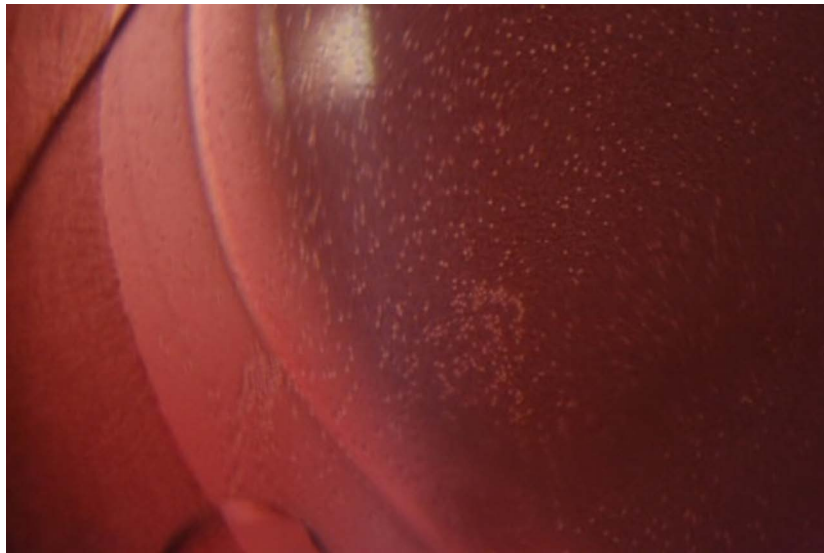


**Fig. 2** Slit lamp images of the LS-313 MF15 lens six months postoperatively  
 Granular deposits were only observed on the LS-313 MF15 lens

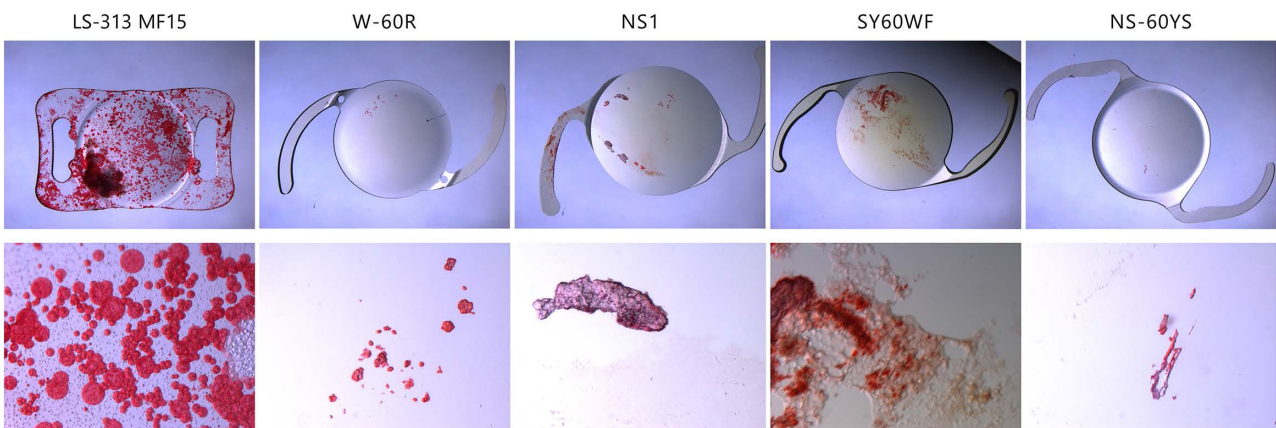


**Fig. 3** Extracted intraocular lenses (IOLs) stained with alizarin red and observed with a stereoscopic microscope  
 The top images were taken at 10 × magnification, and the bottom images at 100 × . The LS-313 MF15 IOLs were stained red all over, with the stains taking a granular appearance, confirming the presence of calcium deposits. Other IOLs also exhibited red stains, whose morphology differed from that of those observed on the LS-313 MF15 IOLs

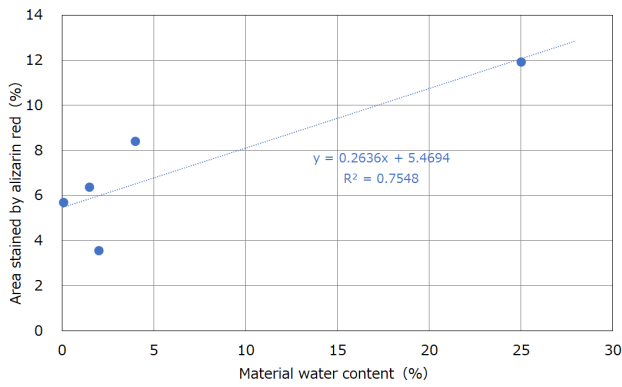


**Fig. 4** Regression line between the water content of each intraocular lens material and the area stained by alizarin red  
The horizontal axis shows the water content of the material, and the vertical axis shows the area stained by alizarin red. A positive correlation was confirmed between the material and the water content. (Correlation coefficient = 0.87)

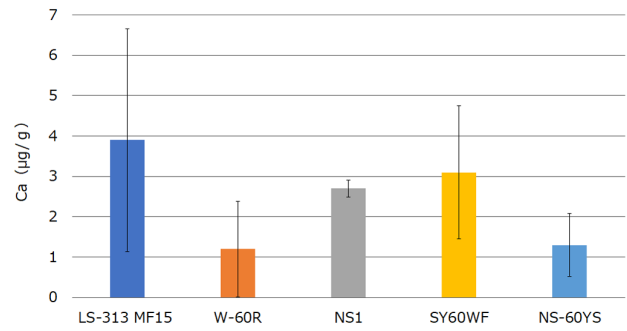


**Fig. 5** Amount of calcium detected in the storage solution of each intraocular lens (IOL)  
All IOLs were stored in physiological saline. The amount of calcium extracted from each storage solution was quantified using inductively coupled plasma mass spectrometry. The highest amount of calcium was detected in the LS-313 MF15 lens storage solution.

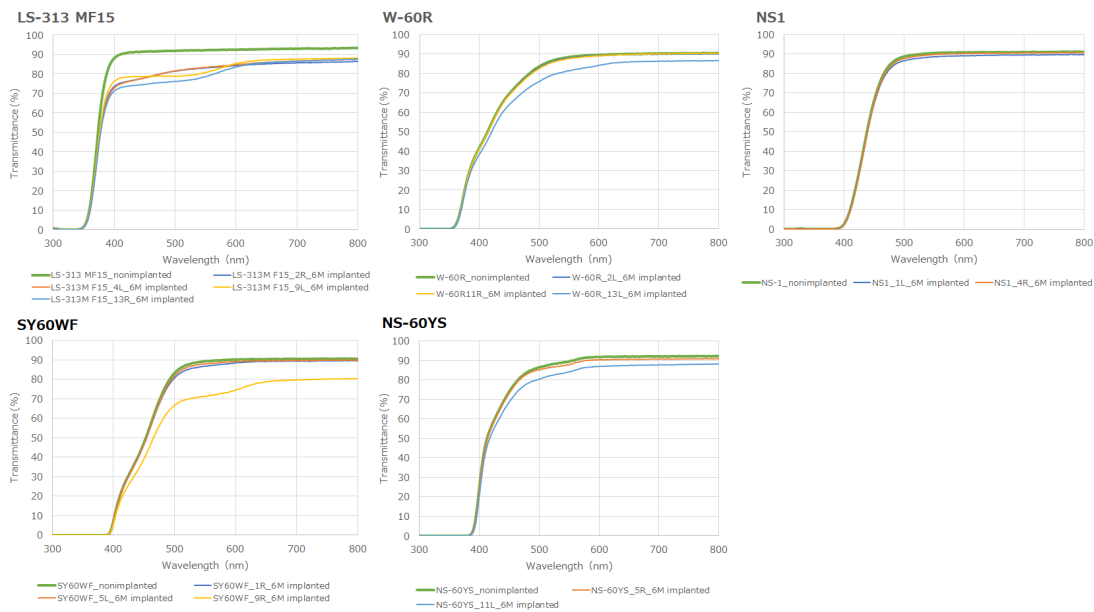


**Fig. 6** Spectral transmission curve of each intraocular lens (IOL)  
The transmittance of non-implanted and excised IOLs at wavelengths of 300–800 nm is shown. Green: Transmittance of non-implanted IOLs. Others: Transmittance of extracted IOLs

**Evaluation of extracted IOLs**

Many cells adhering to the IOLs were extracted from the lens capsule; most cells were removed by ultrasonic washing. The washing time was set at 15 minutes to prevent deposits on the IOL surface from washing away [19].

After washing, the IOLs were stained with alizarin red. The entire LS-313 MF15 IOL surface was stained red, and the locations and morphology matched those of the granular deposits observed using the slit lamp.

Red-stained sites were also identified on the surface of the W-60R, NS1, SY60WF, and NS-60YS IOLs. However, their morphology differed from that of the granular deposits observed on the LS-313 MF15 lenses (Fig. 3).

The proportion of red-stained areas with LS-313 MF15, W-60R, NS1, SY60WF, and NS-60YS IOLs were  $11.9 \pm 13.1$ ,  $8.4 \pm 11.0$ ,  $3.6 \pm 3.3$ ,  $6.4 \pm 3.2$ ,

and  $5.7 \pm 7.9\%$ , respectively. A correlation (correlation coefficient = 0.87) was found between the water content of the material and the dyed area (Fig. 4).

ICP-MS analysis of the storage solution confirmed the presence of calcium during the storage of all IOLs. The amounts of calcium detected in the solutions for LS-313 MF15, W-60R, NS1, SY60WF, and NS-60YS were  $3.9 \pm 2.8$ ,  $1.2 \pm 1.2$ ,  $2.7 \pm 0.2$ ,  $3.1 \pm 1.7$ , and  $1.3 \pm 0.8 \mu\text{g/g}$ , respectively. Thus, the highest amount of calcium was detected in the LS-313 MF15 lens solution (Fig. 5). Furthermore, the transmittance of the extracted lens was measured (Fig. 6), and the rate of decrease in the transmittance of each lens at 500 and 800 nm was calculated (Table 3). The LS-313 MF15 lenses exhibited the highest rate of decrease in transmittance at the 500- and 800-nm wavelengths. The lenses were then divided into two groups: the LS group, comprising the LS-313 MF15 lenses in which

**Table 3** Decrease in transmittance at each wavelength

Model	800 nm	500 nm
LS-313 MF15	$-6.3 \pm 0.8$	$-13.5 \pm 2.7$
W-60R	$-1.7 \pm 2.4$	$-3.8 \pm 4.9$
NS1	$-0.9 \pm 0.6$	$-1.8 \pm 0.7$
SY60WF	$-0.9 \pm 0.2$	$-2.4 \pm 1.2$
NS-60YS	$-2.9 \pm 2.1$	$-4.2 \pm 4.0$

For the transmittance of the extracted intraocular lens (IOL), the fraction of decrease in the transmittance at wavelengths of 500 and 800 nm was calculated as follows: (transmittance of extracted IOL – transmittance of non-implanted IOL)/transmittance of non-implanted IOL). The LS-313 MF15 lenses exhibited the highest rate of decrease in transmittance at both wavelengths.

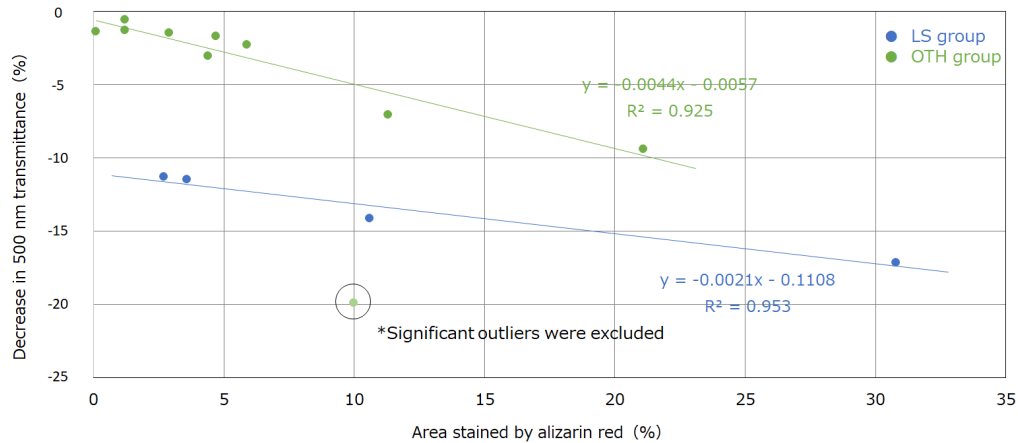


**Fig. 7** Regression line between the decrease in 500-nm transmittance for extracted IOLs and stained area

The horizontal axis shows the area of alizarin red staining, and the vertical axis shows the percent reduction in transmittance at 500 nm (implanted IOL-non-embedded IOL/non-implanted IOL). Blue: LS group: LS-313 MF15. Green: OTH group: W-60R, NS1, SY60WF, and NS-60YS. The correlation coefficient was  $-0.98$  for the LS group and  $-0.96$  for the OTH group, indicating a high negative correlation. However, the regression coefficients were  $-0.0021$  for the LS group and  $-0.0044$  for the OTH group, indicating different tendencies between the two. IOL, intraocular lens; LS group, LS-313 MF15 lenses in which granular deposits were observed; OTH group, other lenses (W-60R, NS1, SY60WF, and NS-60YS) in which no granular deposits were observed

granular deposits were observed, and the other group (OTH group), comprising W-60R, NS1, SY60WF, and NS-60YS lenses, in which no granular deposits were observed. A regression analysis was performed based on the correlation between the area stained with alizarin red and the decrease in transmittance (Fig. 7). However, one of the SY60WF lenses had cells attached to the center of the optical part. This was excluded from the subjects because it was a clear cause of a decrease in transmittance. The decrease in transmittance at 500 nm was affected by the staining of alizarin red. There was a negative correlation between the stained area and the decrease in transmittance. The correlation coefficients were  $-0.98$  and  $-0.96$  for the LS and OTH groups, respectively. Adhesion to the IOL surface resulted in a decrease in the transmittance of the IOL, but the slope of the regression line differed between the LS group and the OTH group. Thus, it was confirmed that the transmittance decreased because of different factors. Furthermore, even at 800 nm, at which IOLs are not easily affected by the staining of alizarin red, LS-313 MF15 lenses had the lowest transmittance. Therefore, it was confirmed that the deposits on the surface contributed to the decrease in transmittance.

## DISCUSSION

Calcium deposition is characterized by calcium phosphate crystals (hydroxyapatite) adhering to the surface of IOLs, causing IOL opacification. It is a serious complication that can occur after cataract surgery, causing glare and visual loss and eventually necessitating the removal and replacement of IOLs [20–23]. Several reports of IOL extraction due to calcium deposition exist, but none have explored the underlying mechanisms in detail. Investigating the principles behind calcium deposition and its elimination to avoid IOL extraction are exceedingly important issues in the development of novel IOL materials.

Previously, opacification observed in the Hydroview H60M lens (Bausch & Lomb), a hydrophilic acrylic IOL, was explained by the adhesion of low molecular-weight silicone sloughed off from the silicone gasket inside the lens case onto the optical surface of the IOL. Long-chain fatty acids within the eye formed calcium and phosphorus deposits upon binding to the low molecular-weight silicone. No clinical reports regarding calcium deposits on Hydroview H60M IOLs have been reported after the gasket was changed from silicone to perfluoroelastomer [24]. Furthermore, in 2014, due to

opacification caused by calcium deposition, Oculentis Corp. initiated a recall of HydroSmart IOLs packaged in glass vials due to the interaction between phosphate crystals used for hydrating the material during the manufacturing process and silicone residues present in a particular batch. Upon changing the packaging to blister packaging, no calcium deposits occurred [25]. These reports suggest that the clinically observed calcium deposition was not caused by IOL materials, but rather by the residual material in the storage container or from the manufacturing process. However, there have been several reports on calcium deposition on IOLs manufactured by Oculentis [26, 27]. Calcium deposition was also reported in the LS-313 MF15 lens used in this experiment [3, 4]. Calcium deposition occurs in hydrophilic IOLs. Thus, materials with a large proportion of hydrophilic components contain factors prone to calcium deposition.

New hydrophobic acrylic IOLs with water content higher than that in conventional hydrophobic acrylic IOLs were developed recently to reduce glistening, with *in vitro* studies and clinical reports indicating good results [9–13]. These IOLs have higher water content than conventional hydrophobic acrylic IOLs due to a higher proportion of hydrophilic components, enabling the IOLs to absorb ions from the aqueous humor, which may eventually lead to calcium deposition on the IOL surface.

Five types of IOLs comprising hydrophilic, new, and conventional hydrophobic materials were selected for this study (Table 1). The LS-313 MF15 lens is a refraction-type rotationally asymmetric +1.5 D-added multifocal IOL that provides good intermediate and distance vision [1]. However, a previous study reported calcium deposition in HydroSmart, a hydrophilic material with a hydrophobic surface comprising hydroxyethyl methacrylate (2-HEMA) and 2-ethoxyethyl methacrylate with 25% water content (the same material as used in LS-313 MF15 lenses) [2, 28].

W-60R, NS1, and SY60WF lenses were selected as new hydrophobic materials. Although the water content of conventional hydrophobic materials is less than 0.4%, materials with higher water content (approximately 1–4% water content) were defined as new hydrophobic materials in this study. The W-60R lens, developed by Advanced Vision Science/Santen using a hydrophobic material, has 4% water content and is stored in 0.9% physiological saline [17]. The NS1 lens has a 2% water content (higher than that of typical hydrophobic materials), exhibiting excellent glistening resistance [16]; it is stored in a sealed pouch. The SY60WF lens has higher (1.5%) water content than the conventional single-piece AcrySof SN60WF (0.4%; Alcon Laboratories, Inc). Furthermore, it has better glistening resistance and long-term stability [9, 29]. The NS-60YS lens was selected as the conventional hydrophobic material, as it has less than 0.1% water content and excellent long-term stability [16]. These IOL materials with different properties were implanted in rabbit eyes to evaluate the effects of calcium deposition on the optical performance and long-term stability of the materials.

## PCO

PCO and migration of residual epithelial cells outside the lens capsule were confirmed in all lenses

in the early postoperative period. Evaluations of PCO in rabbit eyes have been reported previously, but only for observation periods of 1–4 weeks [9, 30]. The lens epithelial cells have a high ability to regenerate in the lens capsule of rabbits; in this observation, the IOL could be maintained in an appropriate state in the lens capsule of rabbits for approximately one month. Subsequently, IOL tilt and anterior chamber collapse due to cell proliferation were confirmed. According to Buchen *et al.* [31], an implantation period of 10 months or more is required to confirm calcium deposition on the hydrophilic IOL in the rabbit model. In this study, IOLs were maintained *in vivo* for as long as possible; however, keratitis and iritis due to rampant PCO were observed. Therefore, an observation period of six months was selected.

At the six-month postoperative follow-up, a large number of cells proliferated in the lens capsule in each lens. The contact between the proliferated cells and the tissue caused hyperemia of the iris and clouding of the cornea. All lenses had severe PCO, but cell proliferation on the LS-313 MF15 lens was slightly less than that of other lenses. No difference was observed between the W-60R, NS1, SY60WF, and NS-60YS lenses in terms of cell proliferation, possibly due to the shape of the haptics of each lens: plate haptics for LS-313 MF15 and C-loop haptics for W-60R, NS1, SY60WF, and NS-60YS. Severe PCO was not observed in rabbit eyes when these IOLs were used clinically. We employed a surgical method identical to that used in human eyes. We performed a CCC (approximately 5 mm), with the opening completely covered by the optical portion of the IOL toward the end of surgery. Nevertheless, the CCC opening could be seen outside the IOL optical portion one week later. Considering the elasticity and cell proliferation ability of the rabbit capsule, it is desirable to set the CCC to approximately 3–4 mm for IOL implantation. According to Bontu *et al.* [30], the PCO observed in rabbit eyes six to eight weeks after implantation was roughly equivalent to that observed after two years in human eyes. For PCO evaluation, the procedure and observation period must be reconsidered.

## Calcification

Granular deposits were confirmed on the IOL surface only in LS-313 MF15 lenses two months postoperatively. The morphology of the deposits differed from that of proliferating cells. Granular deposits were stained with alizarin red.

Gurabardhi *et al.* [32] examined alizarin red-stained IOLs extracted owing to calcium deposition using an optical microscope. The morphology of the calcium deposits was exceedingly similar to that identified in our study. Miyata *et al.* [33] reported that clinical calcium deposition does not occur on all implanted IOLs and that it tends to occur in patients with diabetes or renal dysfunction. The instructions for the LS-313 MF15 lens [34] state that cases involving diabetes, glaucoma, thrombolytic drug use, vitrectomy, and tamponade treatment should be carefully considered due to the likelihood of post-surgical calcium deposition. Kim and Choi [35] investigated calcium and phosphate concentrations in the aqueous humor and serum of cataract surgery patients, and phosphate concentra-

tions were higher in patients with diabetes, particularly among those with proliferative diabetic retinopathy. Furthermore, in the case of glaucoma or vitreous surgery, the protein concentration and components in the aqueous humor differed from those in the case of cataract surgery alone, and they may induce clinical calcium deposition. As a preliminary experiment, we attempted to immerse the IOL material in a saturated calcium phosphate solution. However, we could not reproduce the calcium deposition seen clinically. Calcium deposition on the IOL surface requires the interaction of various factors, such as inflammation *in vivo*, not just the contact of the material with phosphorus or calcium. The ability of the lens epithelial cells to regenerate was very high, and IOL tilt and anterior chamber collapse caused by proliferating cells were confirmed. In addition, it is presumed that iris hyperemia and corneal opacity associated with increased intraocular pressure occurred due to the pressure on the tissue by the proliferating cells. Under such conditions, the components and concentrations in the aqueous humor of the rabbit are presumed to be different from those in normal conditions, and it is presumed that the environment was prone to calcium deposition.

In ICP-MS, calcium was detected in the storage solution of all lenses. However, deposits were observed only in LS-313 MF15 IOLs. Therefore, calcium is adsorbed in all lenses. However, deposits that can be visually recognized are formed only on LS-313 MF15 lenses. It was also confirmed that these deposits reduce the transmittance of the IOL. Thus, the granular deposition we observed was indeed calcium and we were able to reproduce the clinically reported phenomenon of calcium deposition. The granular deposition was observed only on the surface of LS-313 MF15 lenses. Although this occurred under specific conditions, this finding suggests that the risk of calcium deposition cannot be completely avoided simply by changing the IOL shape or manufacturing process. HEMA is prone to calcium deposition [2], and it is presumed that an underlying factor for calcium deposition is present in the material itself. As stated in the instructions for use, the application of LS-313 MF15 should be carefully examined for the risk of calcium deposition in specific cases. In contrast, the stained area of alizarin red tended to increase due to the water content on the surface of the new hydrophobic material, but no granular deposition was confirmed. The introduction of a hydrophilic functional group was expected to impart the properties of a hydrophilic material. However, in this experiment, as with the conventional hydrophobic materials, no calcium deposition was observed. Thus, the introduction of hydrophilic functional groups does not necessarily cause calcium deposition, and it was experimentally proven that the new hydrophobic material has the same low risk of calcium deposition as the conventional hydrophobic material in clinical practice. However, there is a possibility that the water content has a threshold value between 4% and 25%. From the above discussion, we believe that this study provides a useful method to evaluate the potential risk of calcium deposition inherent to the material.

In conclusion, we attempted to reproduce the clinically reported calcium deposition on the surface of plate-haptic rotationally asymmetric refractive multi-

focal IOLs with +1.5 D addition power using rabbit eyes. Granular deposits with a structure similar to that of clinically observed calcium deposits were observed on the surface of LS-313 MF15 IOLs and stained using alizarin red. The granular deposits caused a decrease in transmittance. Although calcium was detected in all five IOLs with varying water content, granular deposits only appeared on the surface of LS-313 MF15 lenses. While rabbit eye results do not always match clinical results, we believe our findings can help in the prediction of calcium deposition on various IOL surfaces in clinical settings and reduce the risk of IOL removal.

## ACKNOWLEDGMENTS

The authors received no financial support for the research, authorship, and/or publication of this article. We would like to acknowledge Kowa Co. Ltd., Hoya Corp., Johnson & Johnson Vision Inc., and Nidek Co. Ltd., who provided IOLs for this study. We would like to thank Editage (<http://www.editage.com>) for English language editing.

## REFERENCES

- 1) Nakajima D, Takahashi H, Kobayakawa S. Clinical outcome of Lentis Comfort intraocular lens implantation. *J Nippon Med Sch* 2021; 88: 398-407. doi: 10.1272/jnms.JNMS.2021\_88-504.
- 2) Gartaganis SP, Prah P, Lazari ED, Gartaganis PS, Helbig H, Koutsoukos PG. Calcification of hydrophilic acrylic intraocular lenses with a hydrophobic surface: laboratory analysis of 6 cases. *Am J Ophthalmol* 2016; 168: 68-77. doi: 10.1016/j.ajo.2016.04.018.
- 3) Safety notice. Santen Pharmaceutical Co., Ltd. Apr 2022, SSI-79. [https://www.santen.co.jp/medical-channel/di/information/2022/DJ180\\_ssi79.pdf](https://www.santen.co.jp/medical-channel/di/information/2022/DJ180_ssi79.pdf). Accessed 1 Jan 2023
- 4) Yildirim TM, Labuz G, Khoramnia R, Son HS, Schickhardt SK, Lieberwirth I, *et al.* Impact of primary calcification in segmented refractive bifocal intraocular lenses on optical performance including straylight. *J Refract Surg* 2020; 36: 20-7. doi: 10.3928/1081597X-20191119-01.
- 5) Werner L, Wilbanks G, Nieuwendaal CP, Dhital A, Waite A, Schmidinger G, *et al.* Localized opacification of hydrophilic acrylic intraocular lenses after procedures using intracameral injection of air or gas. *J Cataract Refract Surg* 2015; 41: 199-207. doi: 10.1016/j.jcrs.2014.10.025.
- 6) Giers BC, Tandogan T, Auffarth GU, Choi CY, Auerbach FN, Sel S, *et al.* Hydrophilic intraocular lens opacification after posterior lamellar keratoplasty – a material analysis with special reference to optical quality assessment. *BMC Ophthalmol* 2017; 17: 150. doi: 10.1186/s12886-017-0546-8.
- 7) Yildirim TM, Khoramnia R, Schickhardt SK, Munro DJ, Merz PR, Son HS, *et al.* Variation in intraocular lens calcification under different environmental conditions in eyes with supplementary sulcus-supported lenses. *Am J Ophthalmol Case Rep* 2020; 19: 100797. doi: 10.1016/j.ajoc.2020.100797.
- 8) Matsushima H, Nagata M, Katsuki Y, Ota I, Miyake K, Beiko GH, *et al.* Decreased visual acuity resulting from glistening and sub-surface nano-glistening formation in intraocular lenses: a retrospective analysis of 5 cases. *Saudi J Ophthalmol* 2015; 29: 259-63. doi: 10.1016/j.sjopt.2015.07.001.
- 9) Werner L, Ellis N, Heczko JB, Ong M, Jain R, Wolfe P, *et al.* *In vivo* evaluation of a new hydrophobic acrylic intraocular lens in the rabbit model. *J Cataract Refract Surg* 2018; 44: 1497-502. doi: 10.1016/j.jcrs.2018.07.040.
- 10) Stanojcic N, O'Brart D, Hull C, Wagh V, Azan E, Bhogal M, *et al.* Visual and refractive outcomes and glistenings occurrence after implantation of 2 hydrophobic acrylic aspheric monofocal IOLs. *J Cataract Refract Surg* 2020; 46: 986-94. doi: 10.1097/j.jcrs.000000000000201.
- 11) Packer M, Rajan M, Ligabue E, Heiner P. Clinical properties of a

- novel, glistening-free, single-piece, hydrophobic acrylic IOL. *Clin Ophthalmol* 2014; 8: 421-7. doi: 10.2147/OPTH.S57114.
- 12) Packer M, Fry L, Lavery KT, Lehmann R, McDonald J, Nichamin L, *et al.* Safety and effectiveness of a glistening-free single-piece hydrophobic acrylic intraocular lens (enVista). *Clin Ophthalmol* 2013; 7: 1905-12. doi: 10.2147/OPTH.S50499.
  - 13) Pagnoulle C, Bozukova D, Gobin L, Bertrand V, Gillet-De Pauw MC. Assessment of new-generation glistening-free hydrophobic acrylic intraocular lens material. *J Cataract Refract Surg* 2012; 38: 1271-7. doi: 10.1016/j.jcrs.2012.02.041.
  - 14) Miyata A, Uchida N, Nakajima K, Yaguchi S. Clinical and experimental observation of glistening in acrylic intraocular lenses. *Jpn J Ophthalmol* 2001; 45: 564-9. doi: 10.1016/s0021-5155(01)00429-4.
  - 15) Kawai K, Hayakawa K, Suzuki T. Simulation of 20-year deterioration of acrylic IOLs using severe accelerated deterioration tests. *Tokai J Exp Clin Med* 2012; 37: 62-5.
  - 16) Kawai K. An evaluation of glistening and stability of intraocular lens material manufactured by different methods. *Eur J Ophthalmol* 2021; 31: 427-35. doi: 10.1177/1120672120902038.
  - 17) Ollerton A, Werner L, Fuller SR, Kavoussi SC, McIntyre JS, Mamalis N. Evaluation of a new single-piece 4% water content hydrophobic acrylic intraocular lens in the rabbit model. *J Cataract Refract Surg* 2012; 38: 1827-32. doi: 10.1016/j.jcrs.2012.05.039.
  - 18) Bompastor-Ramos P, Póvoa J, Lobo C, Lobo C, Rodriguez AE, Alió JL, *et al.* Late postoperative opacification of a hydrophilic-hydrophobic acrylic intraocular lens. *J Cataract Refract Surg* 2016; 42: 1324-31. doi: 10.1016/j.jcrs.2016.06.032.
  - 19) Matsushima H. Opacification of intraocular lens. *J Jan Ophthalmol Soc* 2020; 124: 53.
  - 20) Watanabe J, Akashi M. Novel biomineralization for hydrogels: electrophoresis approach accelerates hydroxyapatite formation in hydrogels. *Biomacromolecules* 2006; 7: 3008-11. doi: 10.1021/bm060488h.
  - 21) Gartaganis SP, Kanellopoulou DG, Mela EK, Panteli VS, Koutsoukos PG. Opacification of hydrophilic acrylic intraocular lens attributable to calcification: investigation on mechanism. *Am J Ophthalmol* 2008; 146: 395-403. doi: 10.1016/j.ajo.2008.04.032.
  - 22) Wu W, Guan X, Tang R, Hook D, Yan W, Grobe G, *et al.* Calcification of intraocular implant lens surfaces. *Langmuir* 2004; 20: 1356-61. doi: 10.1021/la035606q.
  - 23) Drimtzias EG, Rokidi SG, Gartaganis SP, Koutsoukos PG. Experimental investigation on mechanism of hydrophilic acrylic intraocular lens calcification. *Am J Ophthalmol* 2011; 152: 824-33.e1. doi: 10.1016/j.ajo.2011.04.009.
  - 24) Miyakubo H, Miyakubo S. Deposit of calcium on hydrogel intraocular lens and associated factors [in Japanese]. *Jpn J Clin Ophthalmol* 2005; 59: 1505-9.
  - 25) Oculentis GmbH. Urgent field safety notification Oculentis GmbH 2014-001. Voluntary Recall Lentis Hydrosmart Foldable Intraocular Lenses in Glass Vials. 2014. [https://www.hpra.ie/docs/default-source/field-safety-notice/december-2014/v22747\\_fsn.pdf?sfvrsn=2](https://www.hpra.ie/docs/default-source/field-safety-notice/december-2014/v22747_fsn.pdf?sfvrsn=2). Accessed August 25 2022
  - 26) Yamashita K, Hayashi K, Hata S. Toric Lentis Mplus intraocular lens opacification: a case report. *Am J Ophthalmol Case Rep* 2020; 18: 100672. doi: 10.1016/j.ajoc.2020.100672.
  - 27) Neuhann T, Yildirim TM, Son HS, Merz PR, Khoramnia R, Auffarth GU. Reasons for explantation, demographics, and material analysis of 200 intraocular lens explants. *J Cataract Refract Surg* 2020; 46: 20-6. doi: 10.1016/j.jcrs.2019.08.045.
  - 28) Oculentis Internal Data. HydroSmart® – the Innovative Acrylate of the Latest Generation.
  - 29) Kawai K. IOL production methods and long-term stability. *J Jan Ophthalmol Soc* 2020; 124: 53.
  - 30) Bontu S, Werner L, Kennedy S, Kamae K, Jiang B, Ellis N, *et al.* Long-term uveal and capsular biocompatibility of a new fluid-filled, modular accommodating intraocular lens. *J Cataract Refract Surg* 2021; 47: 111-7. doi: 10.1097/j.jcrs.0000000000000391.
  - 31) Buchen SY, Cunanan CM, Gwon A, Weinschenk JI, III, Gruber L, Knight PM. Assessing intraocular lens calcification in an animal model. *J Cataract Refract Surg* 2001; 27: 1473-84. doi: 10.1016/s0886-3350(01)00842-2.
  - 32) Gurabardhi M, Häberle H, Aurich H, Werner L, Pham DT. Serial intraocular lens opacifications of different designs from the same manufacturer: clinical and light microscopic results of 71 explant cases. *J Cataract Refract Surg* 2018; 44: 1326-32. doi: 10.1016/j.jcrs.2018.07.026.
  - 33) Miyata A, Yaguchi S. Participation of low-molecules silicone in calcium deposit on hydrophilic acrylic intraocular lens [in Japanese]. *Jpn J Clin Ophthalmol* 2007; 61: 1555-9.
  - 34) Lentis Comfort, instructions for use. QF2210v2. 2019. <https://lentis-eifu.com/eIFU-Iran/eIFU-QF2210v2-IRN-en.pdf>. Accessed 10 Oct 2021
  - 35) Kim CJ, Choi SK. Analysis of aqueous humor calcium and phosphate from cataract eyes with and without diabetes mellitus. *Korean J Ophthalmol* 2007; 21: 90-4. doi: 10.3341/kjo.2007.21.2.90.